Resonant Raman Transitions into Singlet and Triplet States in InGaAs Quantum Dots Containing Two Electrons

T. Köppen,[1] D. Franz,[1] A. Schramm,[2] Ch. Heyn,[1] D. Heitmann,[1] and T. Kipp[1,*]

[1]*Institut für Angewandte Physik und Zentrum für Mikrostrukturforschung, Universität Hamburg, Jungiusstraße 11, 20355 Hamburg, Germany*

[2]*Optoelectronics Research Centre, Tampere University of Technology, Korkeakoulunkatu 3, 33720 Tampere, Finland*

(Received 12 November 2008; published 14 July 2009)

Semiconductor quantum dots containing two electrons, also called artificial quantum-dot helium atoms, are model structures to investigate the most fundamental many-particle states induced by Coulomb interaction and the Pauli exclusion principle. Here, electronic excitations in quantum-dot helium are investigated by resonant Raman spectroscopy in magnetic fields. We observe transitions from the ground state into the excited singlet state and, in the depolarized Raman configuration which allows spin-flip processes, into the triplet state.

DOI: 10.1103/PhysRevLett.103.037402 PACS numbers: 78.67.Hc, 73.21.La, 78.30.Fs

Spectroscopy on He atoms was one of the fundamental ingredients for the development of the concept of spin and the understanding of exchange interaction. The triplet ortho-He state coined after the experiments of Runge and Paschen in 1895 [1] is a metastable state which is not accessible by dipole excitation from the singlet ground state, the para-He, since this process requires a spin flip. In semiconductor physics, with sophisticated growth techniques it is possible to prepare quantum dots (QDs) which confine a well-defined number of electrons. Doubly charged QDs, which are widely called QD helium because of the analogy to real He atoms, allow us in a most fundamental way to treat and calculate more or less analytically many-electron effects, in particular, the formation of the singlet and triplet states and the impact of exchange effects [2,3]. Like in real He, the transition from the singlet ground state to the excited triplet state is not dipole allowed. In this work, we report on the first direct observation of this singlet to triplet transition in QD He, i.e., the excitation into the ortho-He QD state, by resonant Raman spectroscopy in the so-called depolarized configuration which allows spin-flip processes.

Resonant Raman (or inelastic light scattering) spectroscopy has been successfully applied to investigate the electronic properties of semiconductor nanostructures [4], like ensembles of etched modulation-doped GaAs-AlGaAs QDs [5–11] and also charged self-assembled In(Ga)As QDs [12–14]. In our experiments, we exploit resonances at the fundamental E_0 energy gap of InGaAs QDs in order to enhance the inherently small Raman signals. Doing so, great care has to be taken to distinguish Raman signals from resonant photoluminescence (PL). By analyzing the magnetic-field dispersion, the polarization dependence, and the wave vector dependence we can distinguish between (i) resonant PL transitions, (ii) resonant Raman transitions from the ground state into excited singlet and triplet states, and also (iii) resonant Raman transitions between excited states.

Our samples were grown by molecular beam epitaxy on a GaAs(100) substrate. On top of a GaAs buffer layer and an AlGaAs/GaAs superlattice, a two-dimensional electron system (2DES) of an inverted heterostructure consisting of 30 nm Si-doped AlGaAs, 15 nm AlGaAs, and 40 nm GaAs serves as a backgate. Then, one layer of self-assembled InAs QDs was grown, followed by 33 nm GaAs, 16 pairs of AlAs and GaAs layers (2.5 nm each), and a 7 nm GaAs cap layer. To match the QDs ground-state transition energy with both the sensitivity range of our detector and the emission energy of our laser, we rapidly thermally annealed the samples [15] for 180 s at 740 °C. The nonresonant PL spectrum of this sample [Fig. 1(a)] shows low-temperature ground-state recombination of electrons and holes at 1.308 eV (1.081 eV before annealing). The sequence of emission peaks out of higher excited states prove the total lateral quantization energy for electrons and holes to be about 33 meV. In order to tune the number of electrons in the QDs a 7 nm thick semitransparent Ti gate was deposited on the sample. Separate alloyed contacts were fabricated which connect the 2DES. The occupation of the QDs with electrons can be controlled and monitored by applying a voltage V_g between back contact and gate

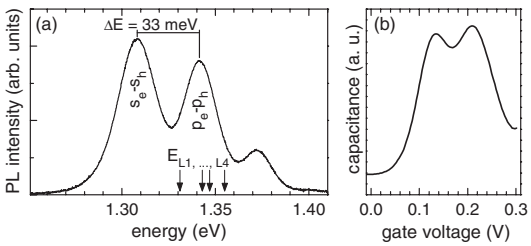

FIG. 1. (a) Nonresonant PL spectrum ($E_L = 1.96$ eV). (b) Capacitance trace under illumination $E_L = 1.343$ eV.

and by measuring the capacitance [16]. Figure 1(b) shows the capacitance trace obtained under laser illumination ($E_L = 1.343$ eV) at low temperature ($T = 9$ K). We observe a subsequent charging of the QDs by two electrons at $V_g = 0.13$ V and at $V_g = 0.21$ V. Unless otherwise noted, all following optical measurements have been performed with $V_g = 0.3$ V when the vast majority of QDs are occupied by two electrons. For optical experiments under resonant excitation the sample has been cooled down to $T = 9$ K in a split-coil cryostat allowing for magnetic fields up to $B = 6.5$ T. A tunable Ti:sapphire laser was focused to a spot size of about 200 μm on the sample. For detection a triple Raman spectrometer equipped with a deep-depletion CCD detector was used.

Figure 2 shows spectra at $B = 4.5$ T for varying excitation laser energies E_L. The energy axis is given in a Raman depiction, i.e., as the difference between E_L and the detection energy E_{det}. We observe several sharp peaks exhibiting different resonance behavior. Roughly, one can say that the peaks labeled T_-, S_-, and T_+ are resonant at lowest E_L. With increasing E_L the peaks labeled T_-^{PL}, Q_1, Q_2, and T_+^{PL} get successively resonant. Figure 3 is the key figure of this work. It shows a compilation of spectra for different magnetic fields for resonant excitation with four different laser energies E_{L1} to E_{L4}, which were chosen close to the resonance of the T and S peaks, the T_-^{PL} peak, the Q peaks, and the T_+^{PL} peak, respectively. The measured intensities are encoded in a gray scale. Regions of different excitation energies are separated by white gaps. Three zones of striking features can be classified. (i) In the energy range from 24 to 42 meV, two strong dispersive branches labeled T_-^{PL} and T_+^{PL} show up when the sample is excited with $E_{\mathrm{L2}} = 1.343$ eV and $E_{\mathrm{L4}} = 1.355$ eV. A third branch labeled S_-^{PL} with comparatively low intensity can be seen for high magnetic fields about 5 meV above the T_-^{PL} branch. A fourth branch labeled S_+^{PL}, which is hardly visible in this depiction but which can be recognized in the single spectra (see Fig. 2), is emphasized by a dashed line. (ii) In the energy range from 13 to 28 meV, four dispersive branches are observed when the sample is excited with the lower laser energy $E_{\mathrm{L1}} = 1.331$ eV. These branches are labeled as T_-, S_-, T_+, and S_+. (iii) In the energy range smaller than 13 meV, further branches show up for $E_{\mathrm{L3}} = 1.347$ eV. Two branches clearly visible for magnetic fields larger than 2 T are labeled as Q_1 and Q_2. A nearly dispersionless branch at about 4 meV is labeled TS. We will show that branches indexed with PL result from resonantly excited PL, whereas all other labeled branches can be assigned to resonant Raman scattering of electronic excitations.

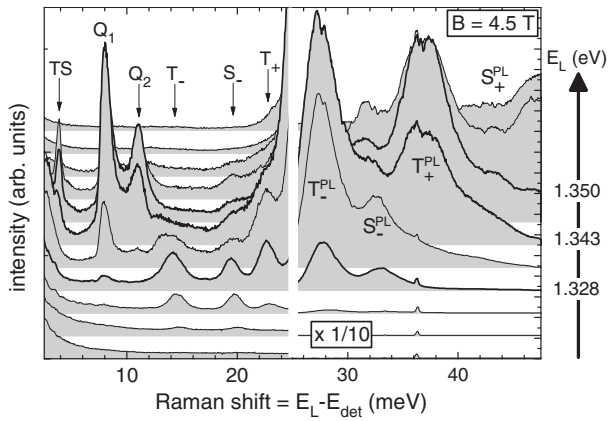

FIG. 2. Spectra obtained at $B = 4.5$ T for laser energies E_L varying between 1.306 and 1.380 eV in steps of ≈ 7 meV. The spectra are vertically shifted and intensities corresponding to energies above 25 meV have been divided by 10. The spectra were taken in polarized configuration.

The energy levels in self-assembled In(Ga)As QDs can be described by assuming a two-dimensional parabolic potential. In a magnetic field this leads to Fock-Darwin single-particle levels for both electrons and holes $E_{nm} = (2n + |m| + 1)\hbar\sqrt{\omega_0^2 + \frac{1}{4}\omega_c^2} + \frac{1}{2}m\hbar\omega_c$ [17]. Here n and m are the radial and angular quantum numbers, respectively, $\hbar\omega_0$ is the quantization energy, and $\omega_c = \frac{eB}{m^*}$ is the cyclotron frequency, with the magnetic field B and the effective mass m^*. ω_0, ω_c, and m^* are different for electrons and holes. Neglecting Zeeman splitting, each single-particle level is twofold degenerate due to the spin degree of freedom. States with $|m| = 0, 1, 2, \ldots$ are called s, p, d, ... Figure 4(a) sketches the single-particle levels for $B > 0$ T.

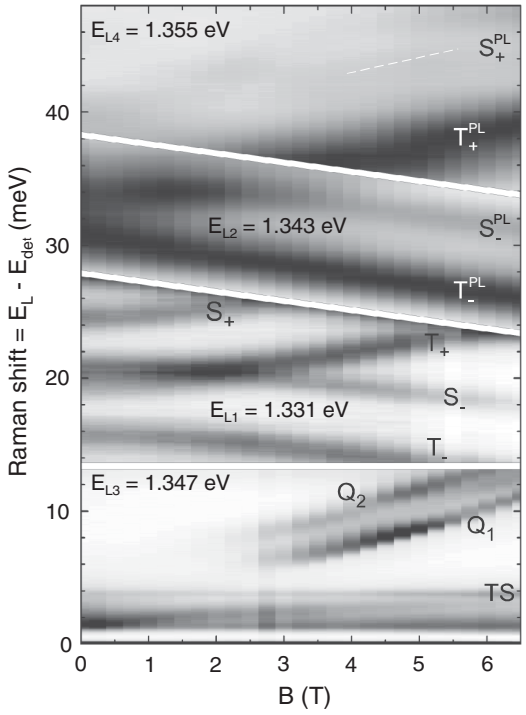

FIG. 3. Compilation of spectra of quantum dots in He configuration for resonant excitation with different laser energies E_{L1} to E_{L4}. Intensities are encoded in a gray scale, the horizontal axis gives the magnetic field B, the vertical axis gives the difference between $E_{\mathrm{L}i}$ ($i = 1, \ldots, 4$) and the detection energy E_{det}. Spectra were taken in polarized configuration.

The indices + and − stand for levels with $m = +1$ and -1, respectively.

Resonant PL.—Exciting with energies near the p_e-p_h transition energy (cf. Fig. 1), electron-hole pairs are resonantly created in the QDs. After excitation, the electron in the p shell cannot relax into the s shell since it is already completely filled with two electrons, whereas the hole quickly relaxes into its s state. After that a radiative recombination process takes place leaving the QDs behind in a configuration with one electron in the s and the other in the p state. Beyond the single-particle picture, if one regards Coulomb interaction, these two electrons form either a singlet or a triplet [2,3], in full analogy to the situation in a He atom. In Fig. 4(b), the described excitation and recombination scheme is sketched in a Fock-Darwin picture for $B > 0$ T involving the p_h^--p_e^- transition (analog for p_h^+-p_e^+). In a finite magnetic field the singlet and triplet states both split into two branches according to the sign of m of the p-shell electron. The recombination process into different final states leads to different emission lines [18,19]. Thus, in our measurement in Fig. 3 where we excite with E_{L2} and E_{L4}, we assign branches T_-^{PL} and T_+^{PL} (S_-^{PL} and S_+^{PL}) to the radiative recombination leaving the triplet (singlet) state behind. For the investigation of an inhomogeneously broadened QD ensemble resonant excitation is inevitable to resolve singlet/triplet splittings in the PL spectra, since the resonance condition automatically selects a subensemble of QDs exhibiting a narrow quantization-length distribution. Such subensembles exhibit only small deviations in the *lateral* quantization which lead for different excitation energies to small shifts of the peaks in their Raman depiction (cf. Fig. 2) [20]. The lateral quantization energy distribution also determines the linewidths of both the PL and the later described Raman peaks. Obviously the T_-^{PL} and T_+^{PL} branches are not degenerated for $B = 0$ T, which can be explained by a slight asymmetry of the lateral potential [21–23].

Resonant Raman transitions from the ground state into excited singlet and triplet states.—The four dispersive branches labeled T_-, S_-, T_+, and S_+ in Fig. 3 resonantly occur for laser energies around $E_{L1} = 1.331$ eV, clearly below the energy of the dipole allowed p_e-p_h transition (cf. Fig. 1). We assign these branches to transitions from the singlet QD helium ground state to excited triplet and singlet states provoked by resonant Raman scattering. Compared to resonant PL branches, they occur about 11 meV closer to the energy E_L of the exciting laser and their intensities are more balanced among each other. Furthermore they show a pronounced polarization dependency, as will be explained later. Descriptively, one may divide the Raman scattering process into two steps, sketched exemplarily for the T_- or S_- branches in Fig. 4(c). First, the laser light resonantly creates a p_e^--s_h electron-hole pair (p_e^+-s_h for T_+ or S_+), then, a radiative s_e-s_h transition occurs, leaving behind the QD in the excited triplet or singlet state. Compared to the resonant PL process, this process fundamentally differs in the absence of the p_h-s_h relaxation, i.e., energy dissipation into the lattice via phonons. Consequently, the excitation step has an energy decreased by the hole quantization energy (11 meV $\approx 33\% \times \Delta E$, cf. Fig. 1). Thus, the Raman process gives directly the excitation energy from the ground state into the excited para- and ortho-He QD state without any ambiguity due to assumptions on the hole confinement energy. From the experimental data at $B = 0$ T we deduce that the transition energy into the triplet state is about 78% of the transition into the singlet state. This is in good agreement to exact many-body calculations after Refs. [2,3], which deliver a ratio of 71% (assuming $\epsilon = 15.15$ and $m^* = 0.075 m_0$).

Importantly, the spectra change drastically if we charge the QDs with one electron ($V_g = 0.16$ V). As depicted in Fig. 5(a), the triplet branches disappear totally, whereas the singlet branches remain. This is consistent with our interpretation since triplet states are many-particle effects and, in a parabolic potential, the single-particle energies are the same as the many-particle center of mass excitation energy due to the generalized Kohn theorem. The spectra of QDs with one electron exhibit strong polaronic contributions [around 14 and 27 meV in Fig. 5(a)] which will be discussed elsewhere.

In contrast to the T^{PL} and S^{PL} branches, the T and S branches show a distinct polarization dependency. In polarized configuration, i.e., when the polarizations of the exciting and the detected light are parallel, the singlet

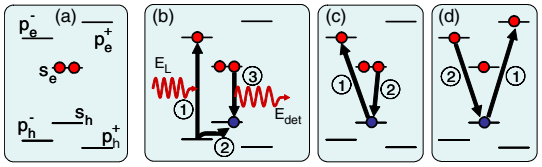

FIG. 4 (color online). Fock-Darwin energy level schemes of QD helium for $B > 0$ T. (a) Ground state. (b) Transition scheme for resonant PL. (c),(d) Schemes of resonant Raman processes.

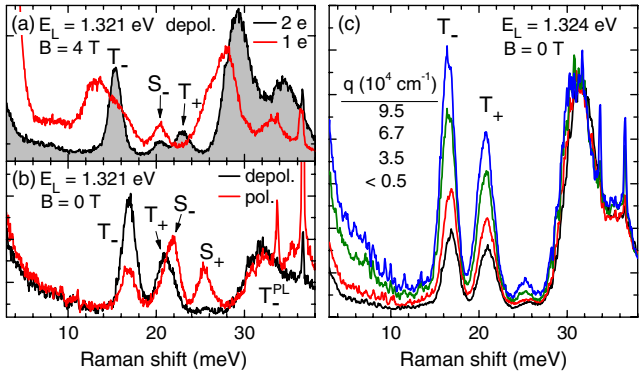

FIG. 5 (color online). (a) Comparison of spectra of QDs containing one and two electrons. (b) Spectra for different polarization configurations. Below (above) 30 meV Raman (resonant PL and phonon) peaks occur. (c) Depolarized spectra for different wave vectors q, normalized to the PL peak at 31 meV.

branches are dominant, whereas in depolarized configuration the triplet branches are enhanced, as can be seen in Fig. 5(b) for $B = 0$ T. It is well known for electronic Raman spectroscopy on QDs that collective charge (spin) density excitations occur in polarized (depolarized) configuration [6–11]. In the QD helium the transition from the singlet ground state to the first excited singlet state is a charge excitation, while the transition to the triplet state—the excitation of the ortho-He QD—is a spin excitation. Thus our experiment is in accordance to the Raman polarization selection rules. We observe a softening of these selection rules for magnetic fields $B > 0$ T, as reported for etched QDs [8,10,11].

The Raman process is a two photon process; thus, in a symmetric system, (dipole) excitations from the ground state to the first excited singlet and triplet states should be forbidden in first approximation because of parity [5,7–10,24]. Since we observe these excitations in backscattering geometry and under orthogonal incidence this selection rule is softened in our QDs. Figure 5(c) shows Raman spectra for $B = 0$ T and $E_L = 1.324$ eV obtained in backscattering geometry but for different incident angles 0°, 15°, 30°, and 45°. The corresponding wave vectors q are given in the figure. The spectra are normalized to the PL peak at 31 meV. Obviously, the Raman peaks can strongly be enhanced by a lateral wave vector transfer, similarly as it has been observed for etched GaAs/AlGaAs QDs with many electrons [5,8].

Resonant transitions between excited states.—Exciting with $E_{\mathrm{L3}} = 1.347$ eV close to the p_h-p_e transition energy leads to resonant occurrence of low energy branches labeled Q_1, Q_2, and TS in Fig. 3. We assign the highly dispersive Q branches to transitions between excited states, from T_- or S_- to T_+ or S_+, for which two resonance conditions have to be fulfilled: First, the excited T_- and S_- states have to be populated resonantly, which occurs for E_{L3} within the resonant PL process described above [cf. Fig. 4(b)]. After that, a resonant Raman process takes place, which can descriptively be divided into the creation of a s_h-p_e^+ electron-hole pair and a subsequent recombination of the p_e^- electron and the s_h hole [see Fig. 4(d)]. This Raman process is only resonant for distinct magnetic fields, for which the s_h-p_e^+ transition energy matches the p_h^--p_e^- transition energy. We assign the Q_1 branch to transitions from T_- to T_+ since it nicely coincides with values obtained by subtracting either branch T_- from T_+ or T_-^{PL} from T_+^{PL}. Q_2 is assigned to transitions from S_- to S_+ since it fits the subtraction of S_-^{PL} from S_+^{PL}. Apparently, Q_1 is more intense than Q_2 (cf. Fig. 2). This is consistent with the above assignment since in average more excited triplet states are occupied than excited singlet states because of the larger degeneracy and the longer relaxation lifetimes of the—metastable—triplet compared to the singlet state [18,25]. Both Q branches do not distinctively follow a polarization selection rule. The nearly dispersionless branch TS in Fig. 3, which occurs at an energy of about 4 meV, is tentatively assigned to transitions between excited triplet and singlet states with similar dispersion, i.e., between ortho- and para-He QD states, from T_- to S_- or from T_+ to S_+. For this resonant transition a hole in a p state is involved instead of a hole in the s state as it is the case in the previously described Raman transitions [cf. Figs. 4(c) and 4(d)].

In conclusion, we report on resonant spectroscopy of ensembles of InGaAs QDs in a varying magnetic field. The QDs contain two electrons, i.e., they are in QD helium configuration. We observe both resonant PL and resonant Raman transitions from the ground state into excited singlet para-He and triplet ortho-He states. The Raman transitions follow the polarization selection rules for charge and spin density excitations. We also observe resonant transitions from afore resonantly excited states.

We thank W. Hansen, U. Merkt, J. Gutjahr, D. Pfannkuche, and C. Schüller for fruitful discussions. We acknowledge financial support by the DFG via SFB 508 and GrK 1286.

*tkipp@physnet.uni-hamburg.de

[1] C. Runge and F. Paschen, Philos. Mag. **40**, 297 (1895).
[2] U. Merkt, J. Huser, and M. Wagner, Phys. Rev. B **43**, 7320 (1991).
[3] D. Pfannkuche, V. Gudmundsson, and P. A. Maksym, Phys. Rev. B **47**, 2244 (1993).
[4] C. Schüller, *Inelastic Light Scattering of Semiconductor Nanostructures*, Springer Tracts in Modern Physics Vol. 219 (Springer, New York, 2006).
[5] R. Strenz *et al.*, Phys. Rev. Lett. **73**, 3022 (1994).
[6] D. J. Lockwood *et al.*, Phys. Rev. Lett. **77**, 354 (1996).
[7] C. Schüller *et al.*, Phys. Rev. B **54**, R17 304 (1996).
[8] C. Schüller *et al.*, Phys. Rev. Lett. **80**, 2673 (1998).
[9] C. P. García *et al.*, Phys. Rev. Lett. **95**, 266806 (2005).
[10] A. Delgado, A. Gonzalez, and D. Lockwood, Solid State Commun. **135**, 554 (2005).
[11] S. Kalliakos *et al.*, Nature Phys. **4**, 467 (2008).
[12] L. Chu *et al.*, Appl. Phys. Lett. **77**, 3944 (2000).
[13] T. Brocke *et al.*, Phys. Rev. Lett. **91**, 257401 (2003).
[14] B. Aslan *et al.*, Phys. Rev. B **73**, 233311 (2006).
[15] S. Malik *et al.*, Appl. Phys. Lett. **71**, 1987 (1997).
[16] H. Drexler *et al.*, Phys. Rev. Lett. **73**, 2252 (1994).
[17] V. Fock, Z. Phys. **47**, 446 (1928).
[18] R. J. Warburton *et al.*, Nature (London) **405**, 926 (2000).
[19] F. Findeis *et al.*, Phys. Rev. B **63**, 121309(R) (2001).
[20] The automatic selection of a distinct subensemble might also lead to an *artificial* magnetic-field dispersion at constant laser energy. We can estimate these deviations to be negligibly small (<0.04 meV/T).
[21] A. Babinski *et al.*, Phys. Status Solidi (c) **3**, 3748 (2006).
[22] S. Hameau *et al.*, Phys. Rev. Lett. **83**, 4152 (1999).
[23] B. A. Carpenter *et al.*, Phys. Rev. B **74**, 161302(R) (2006).
[24] C. Steinebach, C. Schüller, and D. Heitmann, Phys. Rev. B **59**, 10240 (1999).
[25] B. Alén *et al.*, Physica (Amsterdam) **21E**, 395 (2004).